Reprinted from
Jpn. J. Appl. Phys. Vol. 41 (2002) pp. L 294–L 297
Part 2, No. 3A, 1 March 2002

Simplified Monte Carlo Dose Calculation for Therapeutic Proton Beams

Ryosuke KOHNO, Takeji SAKAE[1], Yoshihisa TAKADA, Keiji MATSUMOTO, Hiroyuki MATSUDA, Akihiro NOHTOMI, Toshiyuki TERUNUMA[2] and Yoshikazu TSUNASHIMA[2]

Institute of Applied Physics, University of Tsukuba, 1-1-1 Tennodai, Tsukuba 305-8573, Japan
[1]*Institute of Clinical Medicine, University of Tsukuba, 1-1-1 Tennodai, Tsukuba 305-8575, Japan*
[2]*Proton Medical Research Center, University of Tsukuba, 1-1-1 Tennodai, Tsukuba 305-8575, Japan*

Jpn. J. Appl. Phys. Vol. 41 (2002) pp. L 294–L 297
Part 2, No. 3A, 1 March 2002

Simplified Monte Carlo Dose Calculation for Therapeutic Proton Beams

Ryosuke KOHNO*, Takeji SAKAE[1], Yoshihisa TAKADA, Keiji MATSUMOTO, Hiroyuki MATSUDA, Akihiro NOHTOMI, Toshiyuki TERUNUMA[2] and Yoshikazu TSUNASHIMA[2]

Institute of Applied Physics, University of Tsukuba, 1-1-1 Tennodai, Tsukuba 305-8573, Japan
[1]*Institute of Clinical Medicine, University of Tsukuba, 1-1-1 Tennodai, Tsukuba 305-8575, Japan*
[2]*Proton Medical Research Center, University of Tsukuba, 1-1-1 Tennodai, Tsukuba 305-8575, Japan*

(Received September 13, 2001; revised manuscript received December 26, 2001; accepted for publication December 27, 2001)

A simplified Monte Carlo (SMC) method has been developed for dose calculation of therapeutic proton beams. It uses the depth-dose distribution in water measured by a broad proton beam to calculate the energy loss in a material easily and accurately. It employs the water-equivalent model of inhomogeneous materials. In addition, the multiple scattering effect in the materials is also calculated using the water-equivalent thickness. The accuracy of dose calculations by the SMC method is verified by comparison with dose measurements in a heterogeneous phantom. Results of the measured dose distributions agree well with calculations by the SMC method, though those determined by the dose calculation method based on the pencil beam algorithm show a large discrepancy. Therefore, the dose-calculation method by the SMC method will be useful for application to the treatment planning for proton therapy. [DOI: 10.1143/JJAP.41.L294]

KEYWORDS: proton therapy, proton treatment planning, pencil beam algorithm, simplified Monte Carlo dose calculation, proton dose distribution, heterogeneity, edge-scattering

The conventional dose calculation method using the broad beam algorithm (BBA)[1-3] has been widely used for proton treatment planning because of its simplicity and short calculation time. However, calculation results using the BBA often do not take into account the effect of ray mixing due to multiple scattering of protons in materials.[2]

To improve accuracy, dose calculation methods based on the pencil beam algorithm (PBA) have been developed.[1-7] Dose distribution of the pencil beam is separated into a central-axis term and an off-axis term. The central-axis term is obtained by the broad-beam depth-dose curve measured in water. The off-axis term is described by a two-dimensional Gaussian distribution whose standard deviation is a lateral beam spread which is a function of depth in water. The dose $F(x, y, z; (x_0, y_0))$ from a single pencil beam at an entrance position, (x_0, y_0), is given by

$$F(x, y, z; (x_0, y_0)) = \phi(x_0, y_0) DD(\bar{z}) \frac{1}{2\pi\sigma(z; (x_0, y_0))^2} \times \exp\left(-\frac{(x_0 - x)^2 + (y_0 - y)^2}{2\sigma(z; (x_0, y_0))^2}\right), \quad (1)$$

where $\phi(x_0, y_0)$ is the measured intensity profile of the broad beam at the entrance position of the target, $DD(\bar{z})$ is the depth-dose distribution of the broad beam, $\bar{z}$ is the water-equivalent thickness[8] from the entrance position of the target to the point of interest and $\sigma(z; (x_0, y_0))$ is the lateral beam spread at depth z. We can obtain the dose distribution by generating many pencil beams and by summing the dose distributions over (x_0, y_0).

In previous papers[2,7] we reported the results of experimental evaluation of the PBA for application to proton treatment planning. Results calculated by the PBA agreed well with measured dose distributions in water formed by the proton beam traversing an L-shaped phantom and the calculation time required by the PBA was relatively short. It was suggested that a dose calculation method using the PBA would be useful and applicable to treatment planning for proton therapy. On the other hand, the PBA does not model edge-scattering correctly, thus this calculation method produces errors at the boundary of thick heterogeneous material whose edge is parallel to the beam's central axis.[1]

Since Monte Carlo (MC) calculation methods, such as the well-known GEometry ANd Tracking (GEANT) and Proton Monte Carlo TRANsport program (PTRAN), take into account all physical interactions between particles and materials, application of the MC method which can accurately simulate the edge-scattering effect on proton treatment planning can now be examined. However, the calculation time required by the MC method is considerably long due to the tremendous number of calculations required. In practice, it is too difficult to use such MC codes for dose calculation in routine treatment planning.

In order to improve the situation, a simplified Monte Carlo (SMC) dose calculation method has been developed.[9,10] First, the SMC method uses a measured depth-dose distribution of a broad proton beam in water to calculate energy loss at a given depth. Since the distribution includes energy losses due to electronic stopping and nuclear collisions, energy deposition by secondary particles, loss of primary particles by nuclear interaction and range-straggling effects, dose deposition at a certain depth can be accurately calculated in a short time. We employ a water-equivalent model[8] of heterogeneous materials. Namely, Computed Tomography (CT) numbers obtained by a CT scanner are converted to water-equivalent thickness using a calibrated conversion table. Each voxel of calculation volume is considered to be that of water of different thicknesses. Using the model, calculation of energy loss and scattering is conducted. Matsufuji *et al.* reported that this model is sufficiently accurate to simulate scattering in real tissue.[11] The rms value of multiple Coulomb scattering is calculated by the Highland formula without using a correction factor.[12,13]

To sum up, the SMC method calculates the following two quantities at 1 mm steps in the depth direction for individual proton rays to obtain a dose distribution.

(1) Energy loss using the measured depth-dose curve in water.

*E-mail address: kohno@pmrc.tsukuba.ac.jp

(2) Lateral beam spread due to multiple scattering in water and initial angular spread.

The crucial point is the use of the measured depth-dose curve for calculation of energy losses in materials, which simplifies the calculation yet maintains good accuracy of calculation and reduces calculation time.

Comparison was made among measurements, the PBA and the SMC method. Measurements were carried out using a horizontal beam line at the Proton Medical Research Center (PMRC), University of Tsukuba. Approximately 250 MeV mono-energetic protons are supplied from the High Energy Accelerator Research Organization (KEK) 500 MeV booster synchrotron through a carbon energy degrader and a momentum-analyzing system of the medical beam line.[14] The incident protons were scattered by a 3-mm-thick lead plate (referred to as the first scatterer) to obtain a laterally uniform spatial distribution at a distant position. A binary range shifter of 255 mm thickness was placed between the first scatterer and a patient couch on which we mounted for devices measurement of dose distribution. The residual range of the proton beam traversing them was 90 mm in water.

To measure dose distributions in heterogeneous materials, we manufactured a heterogeneous phantom (200 × 200 × 10 mm) which was made of Tough Water phantoms (TW) and Tough Lung phantoms (TL) produced by Kyoto Kagaku Co., Ltd. The TW is a water equivalent phantom for radiation therapy and the TL is a lung equivalent phantom. The water equivalent thicknesses (WETs) of a slab (10 mm in thickness) of TW and TL are 10.2 and 3.4 mm, respectively. We arranged them to generate a heterogeneous phantom as shown in Fig. 1. The coordinate system is defined in the figure. Since the heterogeneous phantom has an abrupt change of WET in the lateral direction, dose distributions in the phantom are expected to be complicated by edge-scattering effects due to protons passing through the boundary at $x = 0$. The origin of the y-coordinate was defined at the middle of the phantom and the silicon semiconductor detector (SSD) was set at $y = 0$ in this experiment. We measured lateral (x)-dose distributions formed by protons passing through the heterogeneous phantom at intervals of one phantom thickness (10 mm) by scanning the SSD from $z = 12$ to 132 mm.

Figures 2(a) and (b) depict lateral (x)-dose distributions at $z = 72$ and 132 mm obtained by the SSD and results calculated by the PBA and those by one million events in the SMC method, respectively. We normalized the relative dose so that the maximum dose (Bragg peak) of the depth-dose distribution at $x = -40$ mm should be 100%. The error bar represents the relative dose error due to the thickness error of phantoms.

As Fig. 2(a) shows, a dose deposited in the region of

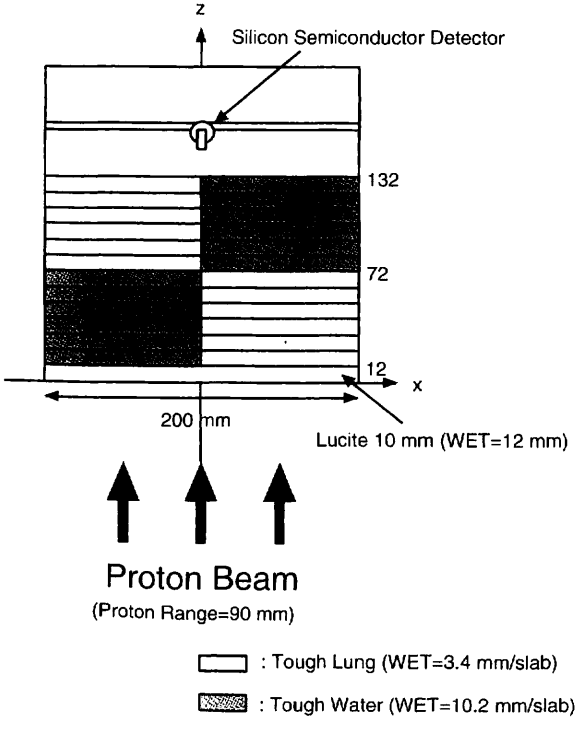

Fig. 1. Experimental arrangement for measurements of dose distributions in heterogeneous materials (plan view).

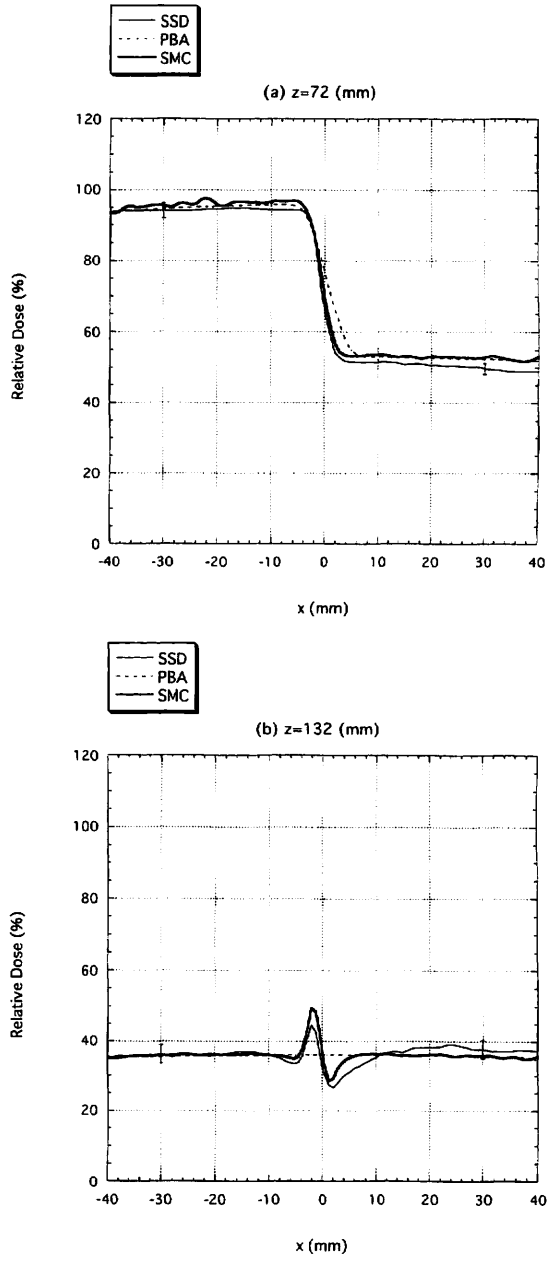

Fig. 2. Comparison of the lateral-dose distributions obtained by the SSD and calculations using the PBA and those by the SMC method at $z = 72$ (a) and 132 mm (b).

$0 \leq x \leq 5$ in the PBA is overestimated as compared with the actual one. This occurs because, for protons scattered from the TW ($x \leq 0$) to the TL ($x > 0$), the dose calculation method using the PBA is calculated as follows: (1) dose contribution at the TL ($x > 0$) from the ray which passes through the TW ($x \leq 0$) is calculated using the central-axis term along the ray which passes through the TW ($x \leq 0$), (2) the scattering effect at the TL ($x > 0$) is the same as that at the TW ($x \leq 0$), though the scattering effect in the TL is actually smaller than that in the TW. On the other hand, the result calculated by the SMC method agrees well with the measured one.

In Fig. 2(b), the result obtained by the SSD indicates the edge-scattering effect in which a bump and dip structure can be seen at approximately $x = 0$. We can explain this phenomenon as follows: (1) protons that scattered in the TW ($x > 0$) out to the TL ($x \leq 0$) have sufficient energy and large energy loss in the Bragg peak region. Thus these protons deposit a relatively large dose at $-5 \leq x \leq 0$. (2) When protons with low energy scatter in the TL ($x \leq 0$) out to the TW ($x > 0$), they lose more energy in the TW than in the TL. Most of them stop in the TW before arriving at $z = 132$ mm. This means that these protons do not contribute to the dose distribution at $0 \leq x \leq 5$. As a result, the dose at $0 \leq x \leq 5$ is relatively low. In short, dose contributions from rays entering the region of $x \leq 0$ and passing into the region of $x > 0$ and vice versa could form a complex dose distribution around the boundary at $x = 0$. From the results, we verified that the dose distributions obtained by the SMC method coincided well with those by the SSD. It was evident that the SMC method could accurately predict the edge-scattering effects which could not be predicted using the PBA.

Figures 3(a)–3(c) show the iso-dose distribution obtained by the SSD and the result calculated using the PBA and that by the SMC method, respectively. The iso-dose curves are drawn for every 10% increase of the relative dose. Figure 3(a) is obtained by interpolating the experimental lateral-dose distributions taken in 10 mm steps in the depth direction. The white region shows that with a dose of more than 90% of the maximum, and the black region shows that with dose less than 10% of the maximum. In spite of this troublesome heterogeneity, the iso-dose distribution obtained by the SMC method agrees well with the experimental result. On the other hand, it is obvious that dose calculation using the PBA produces large errors at approximately $x = 0$.

The program for the calculation is coded by C language on an Alpha-600 MHz computer system. It takes about 20 min to calculate a typical dose distribution formed by one million events.

In conclusion, to apply the Monte Carlo method to proton treatment planning, we developed the SMC method with a new concept in which we only have to calculate two parameters: (1) dose deposition determined by the experimental depth-dose distribution and (2) lateral displacement of protons due to both the multiple scattering effect and the incident proton beam angle. The proton dose distributions determined by the SMC method agree well with the experimental results, though those determined using the PBA could not predict the edge-scattering effect at all. The time required for dose calculation by the SMC is relatively short, thus the dose-calculation method by the SMC will be useful for application to the treat-

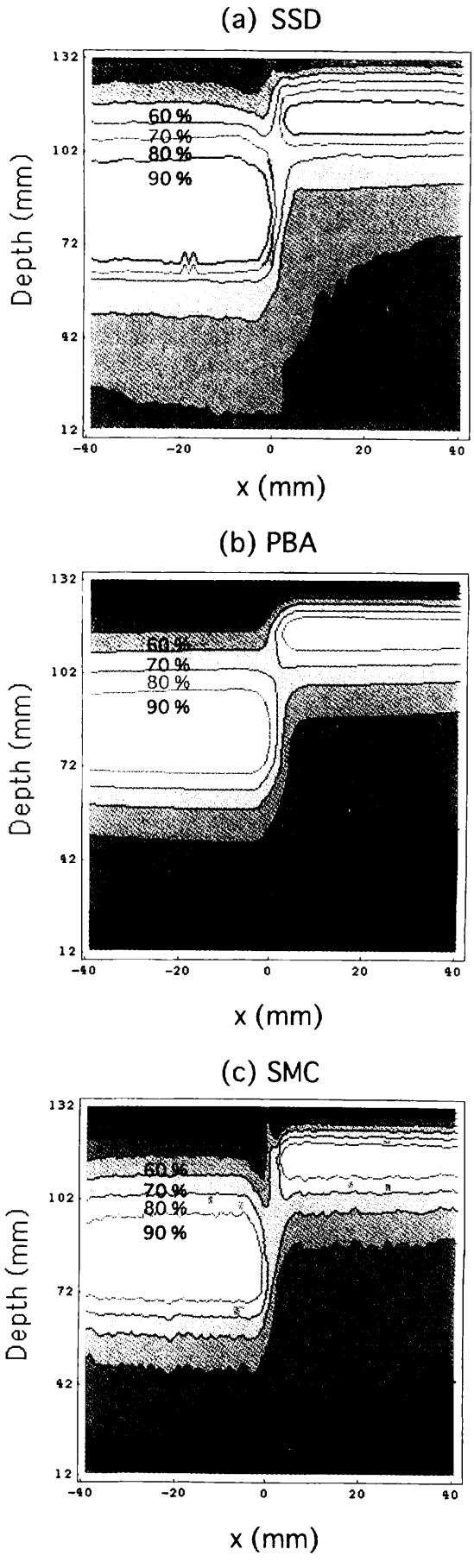

Fig. 3. Comparison of the iso-dose determined by the SSD (a) and by calculations using the PBA (b) and the SMC method (c).

ment planning for proton therapy. Using the SMC, it is possible to omit time-consuming dose distribution measurements required for verification of the bolus configuration designed in treatment planning. Furthermore, it is useful to employ the SMC for designing the bolus in proton treatment planning.

1) L. Hong, M. Goiten, M. Bucciolini, R. Comiskey, B. Gottscalk, S. Rosenthal, C. Serago and M. Urie: Phys. Med. Biol. **41** (1996) 1305.
2) R. Kohno, Y. Takada, T. Sakae, A. Nohtomi, T. Terunuma and K. Yasuoka: Jpn. J. Appl. Phys. **40** (2001) 441.
3) P. L. Petti: Med. Phys. **19** (1992) 137.
4) A. K. Carlsson, P. Andreo and A. Brahme: Phys. Med. Biol. **42** (1997) 1033.
5) B. Schaffner, E. Pedroni and A. Lomax: Phys. Med. Biol. **44** (1999) 27.
6) H. Szymanowski, A. Mazal, C. Nauraye, S. Biensan, R. Ferrand, M. C. Murillo, S. Caneva, G. Gaboriaud and J. C. Rosenwald: Med. Phys. **28** (2001) 975.
7) R. Kohno, Y. Takada, T. Sakae, A. Nohtomi, T. Terunuma, K. Matsumoto and H. Matsuda: Jpn. J. Appl. Phys. **40** (2001) 5187.
8) G. T. Y. Chen, R. P. Singh, J. R. Castro, J. T. Lyman and J. M. Quivey: Int. J. Radiat. Oncology Biol. Phys. **5** (1979) 1809.
9) T. Sakae, A. Nohtomi, A. Maruhashi, M. Sato, T. Terunuma, R. Kohno, Y. Akine, Y. Hayakawa and Y. Koike: Med. Phys. **27** (2000) 368.
10) T. Sakae, A. Nohtomi, M. Sato, Y. Tsunashima, T. Terunuma, R. Kohno and A. Maruhashi: PTCOG XXXIV (2001).
11) N. Matsufuji, H. Tomura, Y. Futami, H. Yamashita, A. Higashi, S. Minohara, M. Endo and T. Kanai: Phys. Med. Biol. **43** (1998) 3261.
12) V. L. Highland: Nucl. Instrum. & Methods **129** (1975) 497.
13) B. Gottscalk, A. M. Koehler, R. J. Schneider, J. M. Sisterson and M. S. Wagner: Nucl. Instrum. & Methods B **74** (1993) 467.
14) D. Kurihara, S. Suwa, A. Tachikawa, Y. Takada and K. Takikawa: Jpn. J. Appl. Phys. **22** (1983) 1599.